Support information

Table S1 *In vitro* binding affinity and half-time of JDTic and LY2456302 at human κ-OR[1-3].

	Receptor binding affinity		$t_{1/2}$ (h) in plasma (PO)	$ratio_{RT(LY2./JDTic)}$
	Ki (nM)	$\Delta G^{exp}_{binding}$[a] (kcal/mol)		
JDTic	0.031	-14.90	About 1.5	2.53
LY2456302	0.807	-12.90	3.8	

[a] $\Delta G^{exp}_{binding}$: calculated from the experimental data via $\Delta G^{exp}_{binding} \approx RT\ln K$ at T = 310 K. The binding energies were calculated based on Ki values.

Table S2 Percentage and average RMSD in angstroms of JDTic/LY2456302 that compose the clusters in the metadynamics simulation.

	JDTic		LY2456302 (60 ns system)	
	Percentage	RMSD	Percentage	RMSD
cluster A	48.6	0.41	35.7	0.61
cluster B	41.4	1.39	36.8	1.53
cluster C	6.2	1.41	2.9	2.14
cluster D	--	--	3.6	3.14
Total	96.2		79.0	

Table S3. The relationship between the LY2456302/JDTic conformations at min/min0/max states and the corresponding cluster these ligands were affiliated in the metadynamics simulation.

	min state	min0 state	max state
LY2456302 system	cluster A1	cluster A4	cluster D
JDTic system	cluster A1	cluster B2	cluster C

Support information

Fig. S1 (A) RMSD calculations of proteins in unbiased JDTic/LY2456302-*κ*-OR systems. (B) RMSF values of all residues from 250 ns to 300 ns in the two systems. (C) Alignment of the final 300 ns JDTic-*κ*-OR frame with initial crystal structure.

Fig. S2 (A) Structural features of LY2456302-*κ*-OR complexes for the cluster B1 (green), cluster C1 (blue) and cluster D1 (pink) during the ligand egress. (B) The variation of the side chain torsion of $Y313^{7.36}$ along the time evolution. (C) Evolution of the distance between N+ in ligands and the conserved residue $D138^{3.32}$ in the metadynamics simulation.

Fig. S3 Metastable states in the additional LY2456302-*κ*-OR system. (A) The binding free energy surface for the dissociation of LY2456302 from *κ*-OR as a function of the Z-component of the vector connecting the nitrogen ion on the pyrrolidine group of the ligand and residue $D138^{3.32}$ and RMSDs of LY2456302. (B) Structural characterization of the two main energy basins B0-B1 in the metadynamics simulation.

Fig. S4 (A/B) Structural features of LY2456302-*κ*-OR (A) and JDTic-*κ*-OR (B) complexes for the min state (green), min0 state (blue) and max state (pink) during the ligand egress.

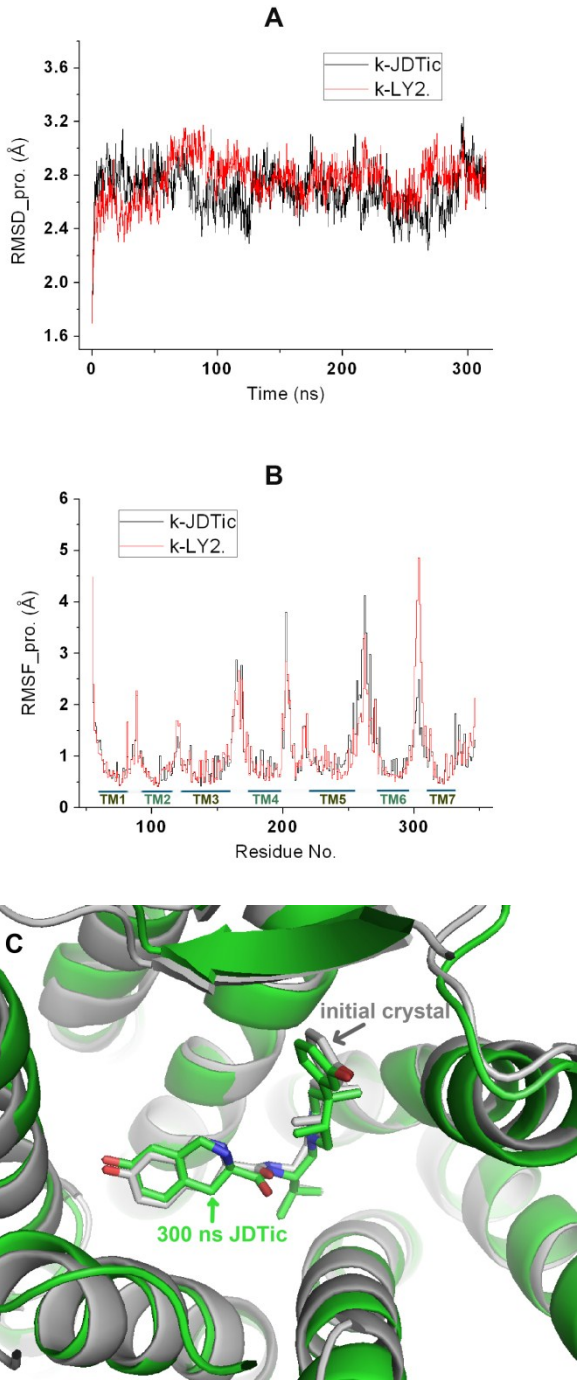

Fig. S1 (A) RMSD calculations of proteins in unbiased JDTic/LY2456302-*κ*-OR systems. (B) RMSF values of all residues from 250 ns to 300 ns in the two systems. (C) Alignment of the final 300 ns JDTic-*κ*-OR frame with initial crystal structure.

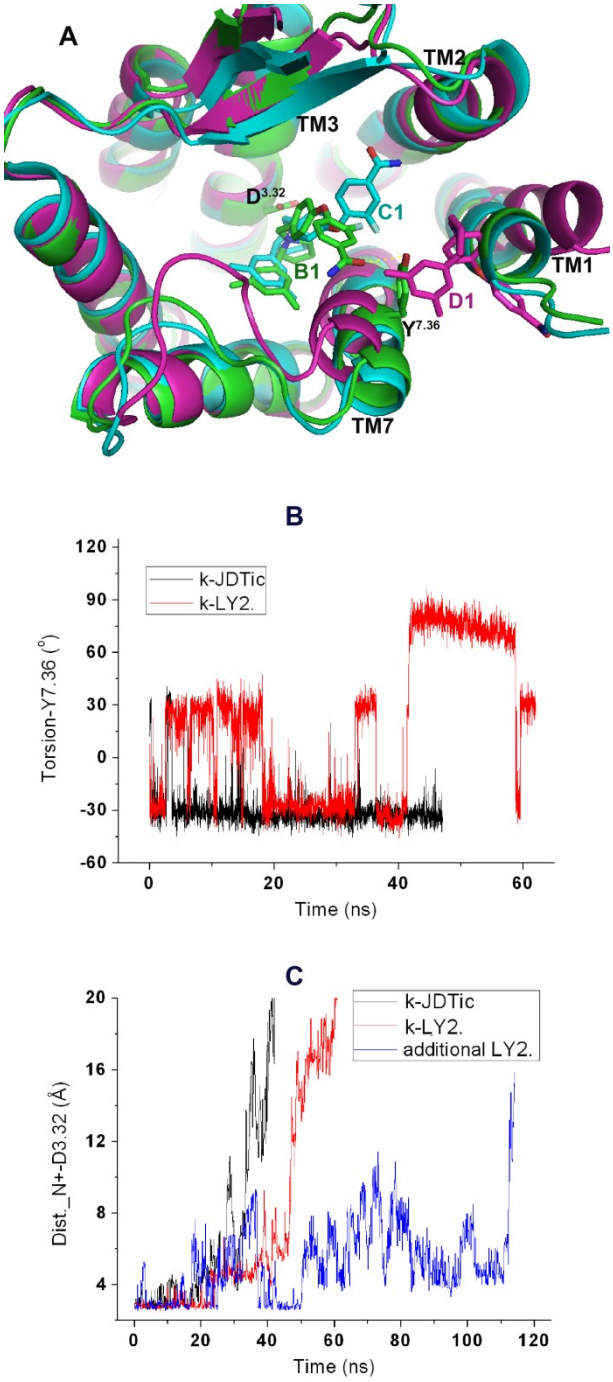

Fig. S2 (A) Structural features of LY2456302-κ-OR complexes for the cluster B1 (green), cluster C1 (blue) and cluster D1 (pink) during the ligand egress. (B) The variation of the side chain torsion of Y313$^{7.36}$ along the time evolution. (C) Evolution of the distance between N+ in ligands and the conserved residue D138$^{3.32}$ in the metadynamics simulation.

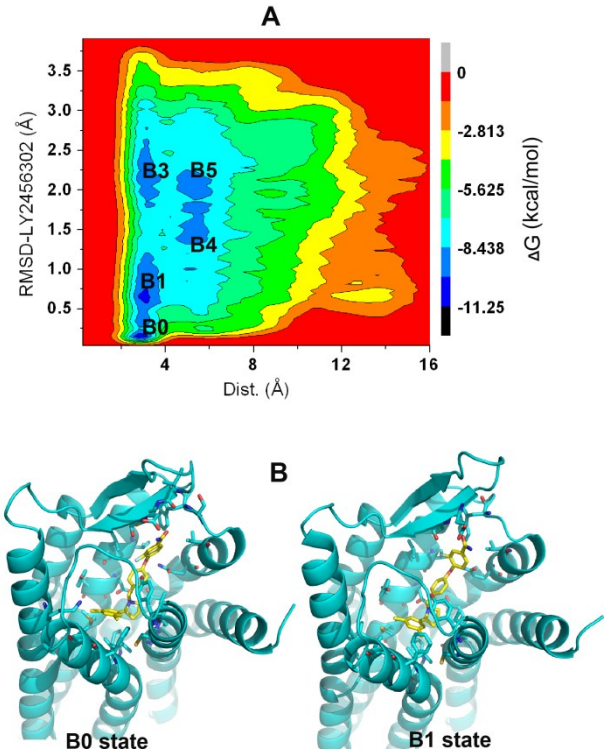

Fig. S3 Metastable states in the additional LY2456302-*κ*-OR system. (A) The binding free energy surface for the dissociation of LY2456302 from *κ*-OR as a function of the Z-component of the vector connecting the nitrogen ion on the pyrrolidine group of the ligand and residue D138$^{3.32}$ and RMSDs of LY2456302. (B) Structural characterization of the two main energy basins B0-B1 in the metadynamics simulation.

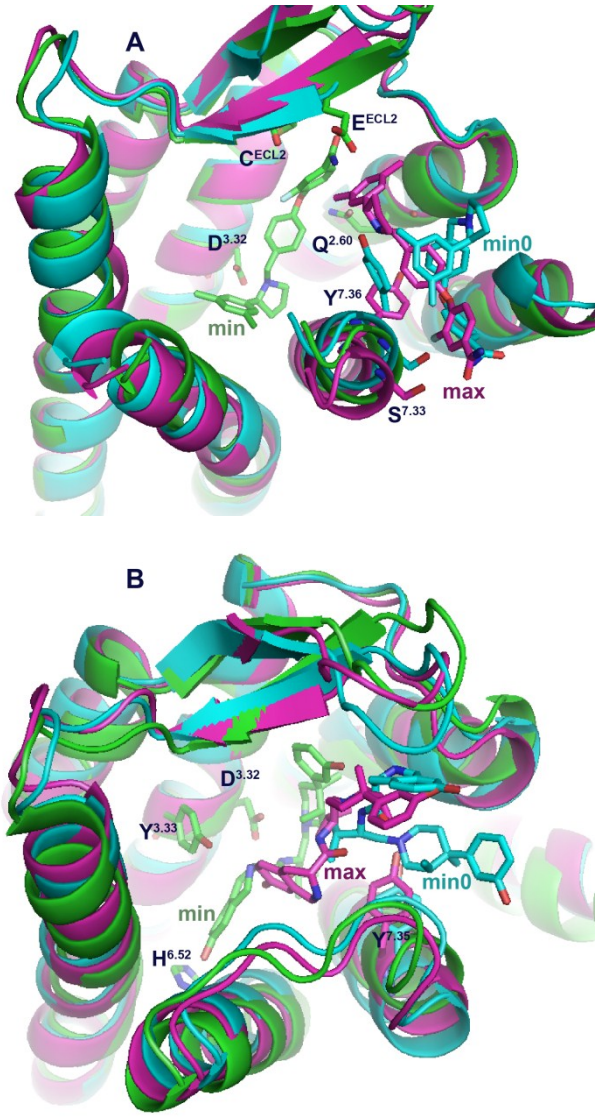

Fig. S4 (A/B) Structural features of LY2456302-*κ*-OR (A) and JDTic-*κ*-OR (B) complexes for the min state (green), min0 state (blue) and max state (pink) during the ligand egress.

Reference:

[1]. Carroll I, et al. Pharmacological properties of JDTic: a novel kappa-opioid receptor antagonist. Eur J Pharmacol, 2004, 501(1-3): 111-119.

[2]. Munro T A, et al. Long-acting kappa opioid antagonists nor-BNI, GNTI and JDTic: pharmacokinetics in mice and lipophilicity. BMC Pharmacol, 2012, 12: 1-18.

[3]. Rorick-Kehn L M, et al. LY2456302 is a novel, potent, orally-bioavailable small molecule kappa-selective antagonist with activity in animal models predictive of efficacy in mood and addictive disorders. Neuropharmacology, 2014, 77: 131-144.